Proceedings of the 28th IEEE
EMBS Annual International Conference
New York City, USA, Aug 30-Sept 3, 2006

Role of Cellular Uncoupling in Arrhythmogenesis in Ischemia Phase 1B

Xiao Jie, Blanca Rodríguez and Natalia Trayanova

Abstract—**Delayed ventricular arrhythmias during acute myocardial ischemia phase 1B are related to a rise in tissue impedance and are most likely sustained in a thin layer of subepicardium. It has been hypothesized that coupling of depressed midmyocardial tissue to the surviving subepicardial layer sets the conditions for reentrant arrhythmias. This hypothesis was verified by means of bidomain simulations on a 3D slab consisting of a normal subepicardial layer coupled to a depressed depolarized midmyocardial layer. The heterogeneity in the coupling was defined by varying the transmural conductivities between the two layers in a circular centrally-located region. The resulting dispersion of effective refractory period in the subepicardium allows for reentry to occur. As uncoupling increases within the circular island, the vulnerability to reentry increases. A higher degree of depolarization in the midmyocardium inhibits the induction of reentry.**

I. Introduction

VENTRICULAR arrhythmias (VA) related to acute ischemia are a major cause of sudden cardiac death. According to experimental results [1], ischemia-induced VA occur in two phases: 1A (2-10 min following coronary occlusion) and 1B (20-30 min). Whereas research has provided significant insight into the mechanisms of arrhythmogenesis in phase 1A, the mechanisms of initiation and sustenance of phase 1B cardiac arrhythmias are still unknown. This delayed phase is more arrhythmogenic since it exhibits an increased incidence of evolved ventricular fibrillation (see reviews in [2]).

During phase 1B, the ischemic midmyocardium is depolarized because of the accumulation of extracellular potassium. Meanwhile, intercellular uncoupling develops as a consequence of increased intracellular calcium concentration ($[Ca^{2+}]_i$) and dephosphorylation of the gap junction proteins [4]. Due to transmural heterogeneity of wall stress and intramyocardial pressure, the subepicardium suffers less cellular damage than the midmural part [3]. Coronel et al. [5] hypothesized that the uncoupling of depressed depolarized midmyocardial tissue to the thin layer of surviving subepicardium leads to dispersion of refractoriness and conduction velocity and therefore provides the substrate for reentrant arrhythmias during phase 1B. Such hypothesis cannot be verified with current experimental techniques since they are unable to provide information about electrical behavior in the depth of myocardium with sufficient spatial resolution.

The goal of this study is to test this hypothesis using state-of-the-art computer simulations of the electrical behavior in ischemia phase 1B. Specifically, the study investigates how vulnerability to arrhythmias is affected by heterogeneities in coupling between the subepicardial and the midmyocardial layers as well as by the degree of depolarization in the inactive layer.

II. Methods

The tissue was modeled as a 30x30x0.7 mm slab (Fig. 1) consisting of a normal subepicardial layer (0.55 mm thickness) coupled to a midmyocardial layer (0.15 mm thickness). The electrical properties of this three-dimensional model were simulated using the bidomain approach [6]. The bidomain model represents the cardiac tissue with both intracellular and extracellular continua, separated by the membrane. The intracellular potential (Φ_i, *mV*) and extracellular potential (Φ_e, *mV*) satisfy the following equations:

$$\nabla \cdot (\hat{G}_i \nabla \Phi_i) = I_m \tag{1}$$

$$\nabla \cdot (\hat{G}_e \nabla \Phi_e) = -(I_m + I_{stim}) \tag{2}$$

where I_m and I_{stim} are the volume density of the transmembrane current and stimulus respectively ($\mu A/cm^3$); $\hat{G}_i$ and $\hat{G}_e$ are the intracellular and extracellular conductivity tensor respectively (*mS/cm*). The inactive midmyocardium was depolarized moderately at a transmembrane potential (V_m) of -86 (normal resting membrane potential), -80, -70 or -60mV. More severe depolarization was not considered because early afterdepolarizations may arise in the subepicardium [11, 12].

Membrane dynamics in the subepicardial layer were represented by the Luo-Rudy dynamic model [8] with modifications from Faber and Rudy [9]. Fibers in the subepicardial layer were oriented parallel to the x axis (Fig. 1) with anisotropic conductivities defined as in a previous study [7]. The resulting ratio between longitudinal and transversal conduction velocities is 1.9, comparable to ~2.1 obtained in experiments (see reviews in [10]).

Two patterns of coupling between the two layers were considered: homogeneous and heterogeneous. In the homogeneous case, the intracellular conductivities in the

This work was supported by AHA Established Investigator Award to Dr. Trayanova, NIH Grant HL63195 to Dr. Trayanova and the EPSRC-funded Integrative Biology e-Science pilot project to Dr. Rodríguez (ref. no: GR/S72023/01).

Xiao Jie and Natalia Trayanova are with the Biomedical Engineering Department, Tulane University, New Orleans, LA 70118 USA (phone: 504-314-2929; fax: 504-862-8779; e-mail: xjie@tulane.edu, nataliat@tulane.edu).

Blanca Rodríguez is with Oxford University Computing Laboratory, Oxford, United Kingdom (e-mail: blanca@comlab.ox.ad.uk).

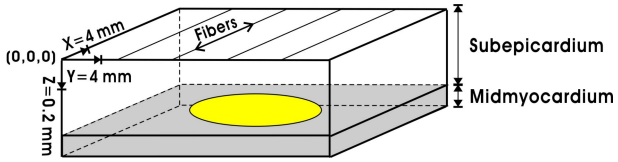

Fig. 1. A schematic illustration of the slab model. The island represents the circular centrally-located region between the layers in the heterogeneously-coupled case.

transmural direction (G_{iz}) between the two layers were uniformly distributed. The degree of coupling is defined as the ratio of G_{iz} over its normal value of 0.19 mS/cm. Three degrees of coupling considered were 0%, 50% and 100%. In the heterogeneous case, coupling between the subepicardium and midmyocardium was decreased to 0% or 50% in a circular centrally-located region of radius 6.6, 7.6, 10.7, 13.1or 14.0 mm (Fig. 1), whereas the coupling outside the island was always normal (i.e. 100%).

To stabilize the ionic currents, the model was paced for five beats from the y=0 surface at a basic cycle length of 250 ms for all cases studied. The stimulus amplitude was of 1.5 times the threshold with 0% coupling between the subepicardial and the midmyocardial layer.

In the homogeneously-coupled model, electrophysiological properties such as action potential duration (APD) and conduction velocity (CV) were evaluated for different degrees of coupling and different levels of midmyocardial depolarization during the fifth pacing stimuli. APD was defined at a specific recording site ((x,y,z) = (15,30,0) mm) from the time of the maximum upstroke slope to 90% repolarization (APD_{90}). CV was calculated as the distance (30mm) over the time required for stimuli to propagate and reach the recording site. Effective refractory period (ERP) was defined as the shortest coupling interval (CI) which allows propagation in the subepicardium following a 6^{th} pacing stimulus.

In the heterogeneously-coupled model, after five pacing stimuli, a premature stimulus (S2) was applied at varying CIs between 60 ms and 120 ms in steps of 1 ms. The vulnerable window (VW) was defined as the range of CIs at which at least one reentrant beat was induced.

All simulations were run on an AMD OpteronTM processor-powered Linux cluster (2.4GHz AMD OpteronTM 250; Advanced Micro Devices, Inc.). The bidomain equations were solved with a Galerkin finite element method [13]. Because the tissue considered was very thin and to reduce the number of elements while assuring certain accuracy, the scale factor in the z direction was set as 2.5 before meshing and then scaled back to its original geometry. The entire mesh consists of 265,458 tetrahedral elements. A semi-implicit backward Euler scheme with variable time steps was employed to solve the time derivatives, as described previously [14]. Convergence tests were conducted by repeating some simulations with finer mesh (doubled the total element number) and smaller time steps (half of original). At the recording site, no difference was found in the APD and changes in activation times were smaller than 3%.

III. Results

Homogeneously-coupled

Fig.2 illustrates the changes in CV, APD, and ERP as the degree of homogeneous coupling and the depolarization in the midmyocardium vary. For all levels of midmyocardial depolarization, increasing coupling between the subepicardial and the midmyocardial layers leads to decrease in CV, APD and ERP. The rate of decrease is much higher from 0% to 50% coupling than from 50% to 100% coupling. Fig. 2 also shows that as the degree of midmyocardial depolarization increases, CV, APD and ERP increase. However, for 0% coupling, CV, APD and ERP are similar regardless of the level of midmyocardial depolarization, since the influence of the depressed midmyocardium is inexistent.

Heterogeneously-coupled

In the heterogeneously-coupled model, application of the premature stimulus during the VW led to the establishment of a reentrant circuit. Fig.3 shows the changes in the VW by varying the subepicardial/midmyocardial coupling inside the island (Fig. 3A), the depolarization level in the midmyocardium (Fig. 3B) and the size of the island (Fig. 3C). VW broadened as the degree of coupling decreased. More depolarization in the midmyocardium narrowed VW. A larger island size increased the vulnerability. The smallest size of the island to induce reentry is 7.6 mm in radius with -70 mV in the midmyocardium.

As an example, Fig. 4 shows the establishment of a figure of eight reentry in the subepicardium following a premature stimulus applied at CI of 105 ms with -70 mV in the midmyocardium and 0% coupling in the island of 13.1 mm in radius (Fig. 4A), compared to no reentrant beat obtained with CI of 110 ms (Fig. 4B). As shown in Fig. 4A, the premature stimulus applied at CI = 105ms elicits a wavefront, which

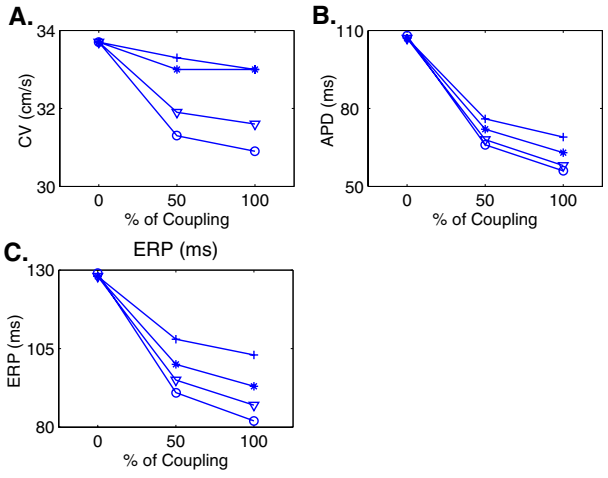

Fig. 2. Changes in CV (**A**), APD (**B**) at the recording site, and ERP (**C**) in the subepicardium as the degree of homogeneous coupling increases. The depressed midmyocardium is of -86 mV (circles), -80 mV (triangles), -70 mV (stars), and -60mV (plus).

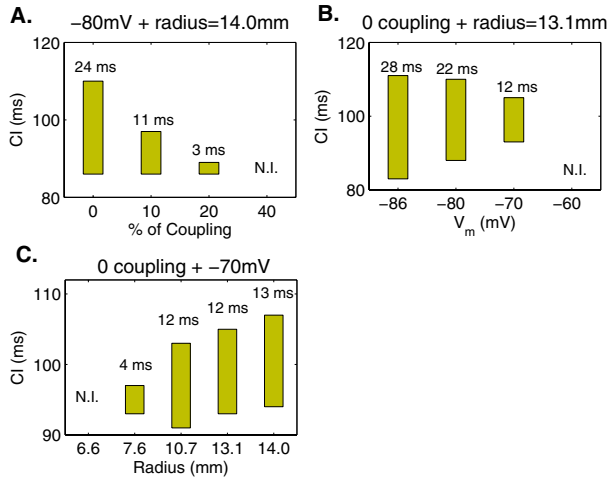

Fig. 3. Vulnerable window (VW) for **A.** varied degree of coupling in the island (radius = 14.0 mm, with -80 mV in the midmyocardium); **B.** varied degree of depolarization (0 coupling in the island, radius = 13.1 mm); **C.** varied radius (0 coupling in the island, with -70 mV in the midmyocardium).

propagates through the normal coupling region, but blocks above the island of uncoupling where refractoriness is extended (T=1.12, 1.14 and 1.16s panels). Eventually, subepicardial tissue above the island recovers allowing reentry of the wavefront, and the establishment of a figure-of-eight reentrant circuit (T=1.18, 1.20, 1.22, 1.24 and 1.26s panels). In contrast, when the premature stimulus is applied at CI=110ms, no reentrant circuit is established (Fig. 4B). When the wavefront initiated by the premature stimulus reaches the island, tissue there has already recovered (T=1.15 and 1.17s panels), and thus no unidirectional block of propagation occurs and no reentrant circuit is established (T=1.19 and 1.21s panels).

IV. Discussions

In this study, we proved that heterogeneous coupling between the normal subepicardial layer and the depressed midmyocardial layer can provide the substrate for arrhythmia induction in ischemia phase 1B by inducing heterogeneities in CV and ERP. The major findings are: 1) Increased uncoupling between the subepicardium and midmyocardium in islands of tissue enhances vulnerability to reentry; 2) A higher degree of depolarization in the midmyocardium inhibits the induction of reentry.

Our results show that coupling between the normal subepicardial and the depolarized inactive midmyocardial layers leads to decrease in subepicardial APD. During action potential (AP), the subepicardium has a higher transmembrane potential than the midmyocardium, and as a result the injury current drawn by the midmyocardium shortens the repolarization phase of the subepicardial AP, which in turn leads to ERP shortening. These results are in accordance with the experimental data [15, 12] obtained by coupling normal individual cells to a simulated depolarized ischemic region with a varied conductance.

Therefore, as an uncoupling island is embedded into the normal coupling interface, APD and ERP are longer in the part of subepicardium directly above the island (region **I**) than outside the island (region **O**). This dispersion of APD and ERP favors reentrant activity. Our simulation results show that heterogeneities in CV due to uncoupling in the islands are small (less than 3 cm/s variation) and play only a secondary role in vulnerability to reentry. This suggests that the electrotonic load from the depressed midmyocardium is not the main reason for slowed propagation [2] in subepicardium during ischemic setup.

As the depolarization in the midmyocardium is increased, both APD and ERP in region **O** increase, but are still shorter than those in region **I**. The decreased dispersion in APD and ERP, in turn, causes the shortening of VW. However, for -60 mV and complete uncoupling within the island (Fig.3B), no reentry can be induced although the dispersion of APD is still considerable (40ms, as evaluated from the homogeneous study, Fig. 2B). This is due to the decreased dispersion of ERP in this case (25 ms, as evaluated from Fig. 2C). Postrepolarization refractoriness (PPR), the difference between ERP and APD, is due to slowing of recovery from inactivation of the fast sodium (Na^+) currents in reigon **O** (results not shown), which is depolarized by the midmyocardium. These results confirmed that although APD is a good indicator of ERP, under ischemic settings, the depression in excitability by depolarization, i.e. PPR, has to be taken into account as well (see reviews in [16]).

Our results also prove that a minimum island size is required to sustain reentry under conditions of heterogeneous coupling between the subepicardial and the midmyocardial layers. If the island is too small, when the time the S2 wavefront reaches region **I**, this region has already recovered from the previous pacing. With full uncoupling in the island and -70 mV in the midmyocardium, ERP is around 128 ms with CV of 33.7 cm/s, thus the predicted smallest pathway of the island is the product of ERP and CV, i.e., 4.3 cm, which is comparable to the simulated result (bigger than 6.6 mm in radius, alternatively, 4.14 cm in circumference, Fig. 3C).

In summary, we have provided mechanistic insights into the role of heterogeneous uncoupling as a substrate for arrhythmogenesis during ischemia phase 1B. Studies have been conducted on the effects of depolarization on individual cells or aggregates [15, 11, 12], but not at a tissue level. Our results can be useful for the development of efficient antiarrhythmic agents. For example, peptides, which can modify the gap junctional conductance, were proposed as potential therapeutic treatment for ischemia-induced arrhythmias [17].

Limitations. Only variations in transmural intracellular conductivities were considered because ischemia 1B is characterized by a rapid increase in intracellular resistances, but extracellular conductivities undergo marked reduction immediately after the ischemic insult and decrease moderately during phase 1B [18]. Other ischemic factors, such as metabolites (K^+, proton etc), may diffuse from the

ischemic region into the subepicardium and may result in tissue depolarization and APD shortening.

ACKNOWLEDGMENT

The authors would like to thank Drs. Ruben Coronel and Joris R. de Groot for valuable discussions, and Rob Blake for his help in computation.

REFERENCES

[1] Kaplinsky E, Ogawa S, Balke CW, Dreifus LS. Two periods of early ventricular arrhythmia in the canine acute myocardial infarction model. Circulation. 1979;60:397-403.

[2] Carmeliet E. Cardiac ionic currents and acute ischemia: from channels to arrhythmias. *Physiol Rev.* 1999;79:917–1017.

[3] Fujiwara H, Ashraf M, Sato S, Millard RW. Transmural cellular damage and blood flow distribution in early ischemia in pig hearts. *Circ Res.* 1982;51:683-93.

[4] Cascio WE, Yang H, Muller-Borer BJ, Johnson TA. Ischemia-induced arrhythmia: the role of connexins, gap junctions, and attendant changes in impulse propagation. *J Electrocardiol.* 2005;38:55-9.

[5] de Groot JR, Wilms-Schopman FJ, Opthof T, Remme CA, Coronel R. Late ventricular arrhythmias during acute regional ischemia in the isolated blood perfused pig heart. Role of electrical cellular coupling. *Cardiovasc Res.* 2001;50:362–372.

[6] Henriquez CS. Simulating the electrical behavior of cardiac tissue using the bidomain model. *Crit Rev Biomed Eng.* 1993;21:1–77.

[7] Eason J, Trayanova N. Phase singularities and termination of spiral wave reentry. *J Cardiovasc Electrophysiol.* 2002;13:672–679.

[8] Luo CH, Rudy Y. A dynamic model of the cardiac ventricular action potential. I. Simulations of ionic currents and concentration changes. *Circ Res.* 1994;74:1071–1097.

[9] Faber GM, Rudy Y. Action potential and contractility changes in [Na(+)](i) overloaded cardiac myocytes: a simulation study. *Biophys J.* 2000;78:2392-404.

[10] Kléber AG, Rudy Y. Basic mechanisms of cardiac impulse propagation and associated arrhythmias. *Physiol Rev.* 2004;84:431-88.

[11] Huelsing DJ, Spitzer KW, Pollard AE. Electrotonic suppression of early afterdepolarizations in isolated rabbit Purkinje myocytes. *Am J Physiol Heart Circ Physiol.* 2000;279:H250-9.

[12] Verkerk AO, Veldkamp MW, Coronel R, Wilders R, van Ginneken AC. Effects of cell-to-cell uncoupling and catecholamines on Purkinje and ventricular action potentials: implications for phase-1b arrhythmias. *Cardiovasc Res.* 2001;51:30-40.

[13] Kwon YW, Bang H. T*he finite element method using MATLAB.* CRC Press, c2000: 37-41.

[14] Trayanova N, Eason J, Aguel F. Computer simulations of cardiac defibrillation: a look inside the heart. *Comput Vis Sci.* 2002;4:259–270.

[15] Tan RC, Osaka T, Joyner RW. Experimental model of effects on normal tissue of injury current from ischemic region. *Circ Res.* 1991;69:965-74.

[16] Burton FL, Cobbe SM. Dispersion of ventricular repolarization and refractory period. *Cardiovasc Res.* 2001;50:10-23.

[17] Pogwizd SM. Prevention of ischemia-induced reentrant ventricular arrhythmias by a peptide that enhances gap junctional conductance. *J Cardiovasc Electrophysiol.* 2003;14:521-3.

[18] Fleischhauer J, Lehmann L, Kléber AG. Electrical Resistances of Interstitial and Microvascular Space as Determinants of the Extracellular Electrical Field and Velocity of Propagation in Ventricular Myocardium. *Circulation.* 1995;92:587–594.

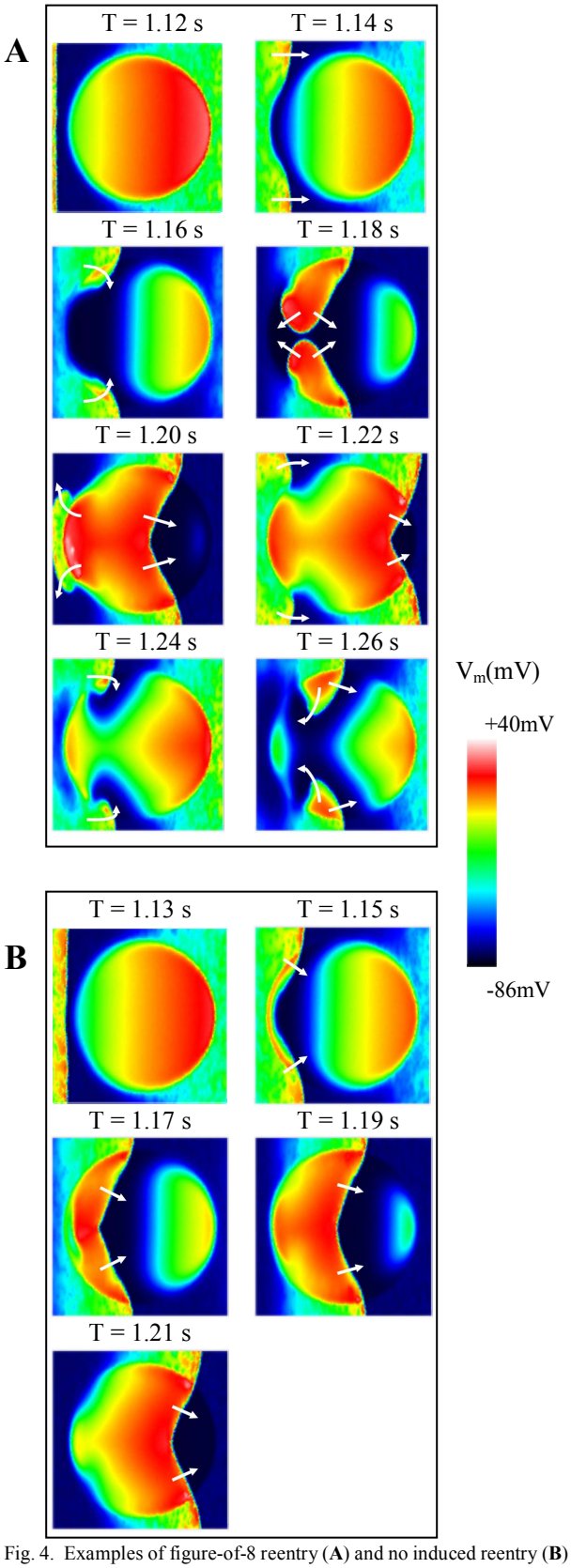

Fig. 4. Examples of figure-of-8 reentry (**A**) and no induced reentry (**B**) in the cross-section of subepicardium (z = 0.45), with -70 mV in the midmyocardium and 0 coupling in the island of 13.1 mm in radius. **A.** CI=105 ms. Time (T) = 1.12 – 1.26 s. **B.** CI=110 ms. T = 1.13 – 1.21 s. Arrows indicate the direction of wave propagation.